The Morris Site 1 Early Navajo Land Use Study:

Gobernador Phase Community Development in Northwestern New Mexico

Volume 2

NNAD Fruitland Data Recovery Series No. 4

Edited by
Douglas D. Dykeman

with contributions by
Douglas D. Dykeman; James K. Feathers, Ph.D.;
John D. Goodman II; Richard G. Holloway, Ph.D.;
Kristin Langenfeld; Pamela J. McBride;
Mollie S. Toll; John A. Torres; Ronald H. Towner, Ph.D.;
Lawrence E. Vogler; and Jeffery T. Wharton

Submitted by
Anthony L. Klesert, Ph.D., Director
Navajo Nation Archaeology Department
P.O. Box 689
Window Rock, Arizona 86515

NM BLM Permits 10-8152-94-6, 10-8152-95-7, and 10-8152-96-8
State Permits 94-036, 94-061, 95-036, 95-061, 96-036, and 96-061

Prepared for

Williams Field Services
San Juan Basin Projects
P.O. Box 1456
Bloomfield, New Mexico 87413

Navajo Nation Papers in Anthropology No. 39

April, 2003

NN028289

Table of Contents

Table of Contents v

List of Figures ix

List of Tables xiii

CHAPTER 7: EARLY NAVAJO LITHIC TECHNOLOGY OF DINÉTAH 191

Introduction 191
Methods and Procedures 191
Lithic Data Collection 191
Lithic Analysis 192
Phase 1: In-field Analysis and Survey Collections—Lithic Data Summary 194
Chipped Stone Artifacts 194
Phase 2: Excavations of LA 11196 and LA 88766—Lithic Data Summary 212
LA 11196 Lithic Data Summary 212
LA 88766 Lithic Data Summary 217
Phase 3: Focused Data Recovery—Lithic Data Summary 218
Chipped Stone Artifacts 219
Battered Tools 219
Milling Implements 219
Ground Tools 219
Interpretation and Summary 220
Lithic Data Synthesis 221
Intersite Variability 221
Lithic Landscape Management 221
Early Navajo Reductive Technologies 226
Early Navajo Productive Technologies 227
Summary 231

CHAPTER 8: POTTERY OF THE MORRIS SITE 1 EARLY NAVAJO LAND USE STUDY 233

Introduction 233
Phase 1 Results: On-site Analysis and Collections Analysis 235
Phase 2 Results: Excavations at LA 11196 and LA 88766 236
LA 11196 236
LA 88766 257
Phase 3 Results: Midden Testing 258
The Data Set 259
Characteristics of the Assemblages 259
Vessel Counts and Midden Size Estimates 262
Summary 265
Consideration of the Research Questions 266
Association of Pottery by Site Type 266
Ceramic Diversity and Site Type 268
Pottery Assemblages on Habitation Sites 272
Pottery and Feature Function 275
Glaze Ware in the Morris Site 1 Project Area 280
The Origin and Characteristics of Gobernador Polychrome 285
Gobernador Polychrome in Early Navajo Households and Society 289
Summary and Concluding Remarks 291

NN028290

CHAPTER 9: VERTEBRATE FAUNAL REMAINS 297
Research Orientation 298
Effective Ecology 299
Faunal Analysis Perspectives 300
Analysis Procedure and Terminology 301
LA 11196 Results 302
Interpretive Summary 303
LA 79456 Results 303
Interpretive Summary 304
LA 83529 Results 304
Interpretive Summary 305
LA 105428 Results 305
LA 105530 Results 305
Interpretive Summary 306
LA 105630 Results 306
LA 105930 Results 307
Interpretive Summary 307
LA 106199 Results 307
Interpretive Summary 308
LA 106203 Results 308
Interpretive Summary 309
Species Descriptions and Ethnohistoric Data 310
Order Artiodactyla (Even-Toed Mammals) 310
Family Cervidae (Elk, Moose, Caribou, Deer) 310
Family Bovidae (Cattle, Sheep, Goats, Old World Antelope) 311
Order Perissodactyla (Odd/Even-Toed Mammals), Family Equidae 313
Order Lagomorpha (Rabbits, Hares, and Pikas) Family Leporidae (Rabbits and Hares) 313
Order Rodentia (Mice, Squirrels, and Allies) 314
Suborder Myomorpha, Family Cricetidae (Deer Mice, White-Footed Mice, Woodrats, and Allies), Subfamily Cricetinae (Cricetine Mice and Rats) 314
Class Reptilia 315
Order Squamata, Suborder Sauria (Lizards), Family Iguanidae 315
Interpretations and Conclusions 315

CHAPTER 10: FLORAL COMPONENTS OF EARLY NAVAJO LAND USE: THE MORRIS SITE 1 COMMUNITY 319
Introduction 319
Methods 319
Results 320
LA 11196 320
LA 88766 320
Discussion: Early Navajo Plant Use In The Four Corners Area 320
Summary 321

CHAPTER 11: POLLEN ANALYSIS OF NAVAJO PERIOD SAMPLES FROM THE MORRIS SITE 1 PROJECT 325
Introduction 325
Methods and Materials 325
Palynological Extractions 325

NN028291

Results 327
LA 88766 327
LA 11196 328
Discussion 330
Conclusions 333

CHAPTER 12: DENDROCHRONOLOGY IN THE MORRIS SITE 1 PROJECT AREA .. 335

Introduction 335
Research Domains 335
Tree-Ring Dating Theory and Interpretation 341
Formation Processes of Tree-Ring Dates 342
Heartwood/Sapwood Issues 342
The Approach Used Here 344
Methods 345
Field Sampling Procedures 345
Identifying Dateable Samples 345
Distinguishing Axe Marks 345
Laboratory Sample Analysis 346
Dendrochronological Results 346
Cumulative Date Distributions 346
Individual Site Analysis 349
Wood Use 353
Methodological Considerations 354
Discussion 355
Conclusions 356

CHAPTER 13: THERMOLUMINESCENCE DATING OF EARLY NAVAJO CERAMICS 357

Field Collection Methods 357
The TL Technique 357
Derivation of TL Dates 358
Procedures 358
Results 359
Ages 363
Discussion and Conclusions 363

CHAPTER 14: TREE RINGS AND THERMOLUMINESCENCE: CHRONOLOGY AND DATING ISSUES OF THE EARLY NAVAJO OCCUPATION 373

The Problem 373
Tree Ring Dates 375
Thermoluminescence Dates 376
Tree-Ring and TL Correlation 380
Direct Comparison 381
Aggregate Comparison 385
Thermoluminescence and Archaeological Dating 385
TL and Radiocarbon 385
TL and Ceramics 387
Conclusions 388

NN028292

CHAPTER 15: EARLY NAVAJO SETTLEMENT AND LAND USE 391
Time and Population, a Control for Settlement Analysis 391
Modeling Population 391
Settlement Pattern 398
Patterning in Site Distribution 401
Residential Patterning 406
Summary and Conclusions 414
Land Use 415
Landform and Settlement 415
Settlement Pattern and Resources 421
Summary and Conclusions 426

CHAPTER 16: THE EARLY NAVAJO COMMUNITY 427
Elements of Community in the Morris Site 1 Project 427
Economic Organization 427
Sociopolitical Organization 433
Religious Organization 441
Pueblito in the Community Context 443
Pueblito Architecture 443
Types of Pueblitos 443
Discussion 446
Frances Mesa Community: A Socioeconomic Perspective 447
Conclusions 450
Navajo Community, an Enduring Tradition 452

REFERENCES CITED: VOLUME 2 455

Appendix G: Lithic Assemblage Data

Appendix H: Obsidian Sourcing Analysis

Appendix I: Ceramic Analysis Methods

Appendix J: Ceramic Assemblage Data

Appendix K: LA 11196 Vessel Descriptions

Appendix L: Puebloan Glazeware Ceramics

Appendix M: Gobernador Polychrome Designs

Appendix N: Trade Ware Pottery Designs

Appendix O: LA 11196 Flotation Results, LA 88766 Flotation Results, Wood Species Composition, Macrobotanical Materials

Appendix P: Pollen Data, Principal Components Analysis, Simpson's Diversity Index

Appendix Q: Explanation of Symbols Used for Reporting Tree-ring Dates

Appendix R: Pueblito Data

NN028293

CHAPTER 13: THERMOLUMINESCENCE DATING OF EARLY NAVAJO CERAMICS

by James K. Feathers

The original intent of the chronology problem domain of the Morris Site 1 data recovery plan was to explore ways to improve the dating success and accuracy of early Navajo period sites. Thermoluminescence (TL) dating appeared to be a good method to do this because it can be used to date a variety of cultural materials that are common on early Navajo sites. Moreover, the technique can date materials from both surface and subsurface contexts, thereby offering the possibility of absolute dating results while minimizing impact to archaeological sites. One problem with TL dating was that few dating results were available and its utility was unproven in Southwestern archaeology. Consequently, TL dating was regarded with skepticism by archaeologists (e.g., Reed and Horn 1990). In order to gain some confidence in the TL technique, a comparison of TL and tree-ring dates was proposed in the data recovery plan. This necessitated implementation of a TL sampling program that was both intensive and extensive in the Morris Site 1 project area. Intensive sampling served to test the internal consistency of resultant suites of TL dates and extensive sampling distributed the dated site population throughout the project area, thereby indicating the duration and extent of the Navajo occupation.

Field Collection Methods

Extensive TL sampling was performed during the archaeological inventory phase. This entailed the collection of surface samples, primarily ceramic sherds and burned rock, suitable for TL dating purposes. The sample was heavily weighted toward ceramic sherds, because these were subjected to kiln temperatures sufficient to set the TL signal and, when properly type classed, sherds represented unambiguous association with the targeted early Navajo occupation. The primary criteria for ceramic sherd sample suitability were size and thickness. The minimum requirements were 3 cm in diameter and at least 5 mm in thickness.

Intensive sampling of TL dates was accomplished during the focused data recovery and excavation phases of the project. In fact, the primary objective of the focused data recovery was the collection of TL samples from subsurface contexts. These samples were to serve as controls in the event that the surface samples did not produce reliable dates due to uncertainties in the external dose rate. The criteria for sample suitability were the same as described for TL samples obtained by the archaeological inventory.

Collection of TL samples during all phases of the project resulted in more samples than could be dated with the available resources. Consequently, the final selection of TL samples for dating was a complex process that involved several criteria. The foremost criteria were even distribution in the project area, association with tree-ring dates or other TL dates, and sample suitability for TL dating. An even distribution of dated TL samples was desired to account for potential temporal variation in the Navajo settlement pattern. Some samples were selected for contextual association with other dates. This allowed for direct comparison of TL and tree-ring dates, or in the case where multiple TL dates were reported from the same site, the consistency of the TL dates could be evaluated.

Because long range gamma radiation is a significant contributor to the luminescence signal, accurate estimation of the external dose rate is required to obtain accurate dates. Commonly, the radioactivity of a soil sample collected adjacent to the ceramic is measured for this purpose. Where the environment is rather heterogeneous, an advisable check is to measure the external dose rate *in situ* by placing dosimeters at the find location. Four dosimeters were placed during the focused data recovery phase and left for one year, as described in chapter 6. Results are presented in this chapter.

The TL Technique

Thermoluminescence dating is based on the accumulation of stored energy that occurs in some crystalline materials as a function of natural radioactivity. This energy may be released as light (luminescence) when exposed to sufficient heat, which in effect acts as a zeroing mechanism. The intensity of the luminescence signal, measured by heating in the laboratory, is proportional to the amount of stored energy, which in turn is proportional to the amount of absorbed radiation. If the radiation dose rate is a constant function of time, the luminescence intensity can then be related to the time since the last zeroing event

NN028294

(exposure to heat). Since the major sources of natural radioactivity are radionuclides with exceptionally long half-lives, a constant dose rate can be assumed, except where geological processes have altered the radioactive concentrations. The latter situation can often be detected and sometimes corrected.

The following expression is used to derive ages in luminescence dating:

$$\text{Age}(t) = D_E\,(\text{Gy}) / D_R\,(\text{Gy/t}).$$

D_E is the equivalent dose (measured in Gy, or grays, the unit of absorbed radiation), which is the amount of radiation equivalent to what was necessary to produce the sample's natural luminescence signal. D_R is dose rate (in Gy per unit time, t). D_E is measured by calibrating luminescence sensitivity against artificial irradiation applied in the laboratory. It requires isolating signals that have been thermally stable over time and which increase with applied radiation. The dose rate is the sum of alpha, beta, gamma, and cosmic dose rates in the sample and its immediate environment.

The last heating event for prehistoric pottery is usually its manufacture or use, both of which correspond to events of archaeological interest. TL dating thus provides direct dates that do not require bridging arguments linking the dating event with the target event. Bridging arguments are required to use tree-ring dates to estimate the time of ceramic manufacture or use, since tree-rings do not date a ceramic event. Underestimations in age by TL are possible if the ceramic was heated postdepositionally, for example, by a forest fire, but such occurrences are not common and often detectable.

TL also can be applied to heated stones, for example, those used in hearths, provided the stones have been heated sufficiently (at least 450-500°C). Luminescence can also date buried sediments, which is usually done by the related technique of optically stimulated luminescence (OSL).

Derivation of TL Dates

Procedures

The following procedures were used for the TL analysis. This is a generalized procedure for the laboratory, written in present tense. Where specific procedures deviated some language in past tense has been added.

Sample Preparation

The sherd is broken to expose a fresh profile. Material is drilled from the center of the cross-section, more than 2 mm from either surface, using either a tungsten carbide or stainless steel drill tip. The material retrieved is ground gently by a corundum mortar and pestle, treated with HCl, and then settled in acetone for 2 and 20 minutes to separate the 1-8 μm fraction. This is settled onto a maximum of 72 stainless steel discs.

For two of the inventory samples, instead of drilling, the outer 2 mm were removed by a diamond saw and the remaining interior crushed with a vice. An attempt was also made to remove coarse quartz grains (90-125μm) from these but in both cases only a very small amount of suitable material was extracted. Some single aliquot OSL analyses were attempted, but the results were not consistent and no further effort was made to date the samples in this way.

For one of the sandstone samples in the excavation samples (UW253), 90-125μm quartz grains were used. These were obtained by removing the outer 2 mm as above and then sieving the crushed material through nested screens. The 90-125μm fraction was treated with HCl, etched with HF for 40 minutes, rescreened, and then density separated using a 2.67 specific gravity solution of sodium polytungstate. For the other sandstone sample (UW254), little material in the 90-125μm fraction was available, so a 73-90μm fraction was used instead. This fraction was not etched or density separated, and probably included some feldspar as well as quartz. Dosimetric corrections for the grain size were made.

Glow-Outs

Thermoluminescence is measured by a Daybreak reader using a 9635Q photomultiplier with a Corning 7-59 blue filter, in N_2 atmosphere at 1°C/s to 450°C. A preheat of 240°C with no hold time precedes each measurement. Artificial irradiation is given with a ^{241}Am alpha source and a ^{90}Sr beta source, the latter calibrated against a ^{137}Cs gamma source. Discs are stored at room temperature for one week after irradiation before glow out. Data are collected by a multi-channel analyzer and processed by Daybreak TLApplic software.

For the inventory samples, a preheat of 70°C for three to seven days was used instead of the 240°C preheat.

Fading Test

Several discs are used to test for anomalous fading. The natural luminescence is first measured by heating to 450°C. The discs are then given an equal alpha irradiation and stored at room temperature for varied times: 10 minutes, 2 hours, 1 day, 1 week, and 8 weeks. The irradiations are staggered in time so that all of the second glows are performed on the same day. The second glows are normalized by the natural signal and then compared to determine any loss of signal with time (on a log scale).

For the inventory samples, maximum storage was only for three weeks but at 70°C.

NN028295

Equivalent Dose

The equivalent dose is determined by a combination additive dose and regeneration (Aitken 1985). Additive dose involves administering incremental doses to natural material. A growth curve plotting dose against luminescence can be extrapolated to the dose axis to estimate an equivalent dose, but for pottery this estimate is usually inaccurate because of errors in extrapolation due to nonlinearity. Regeneration involves zeroing natural material by heating to 450°C and then rebuilding a growth curve with incremental doses. The problem here is sensitivity change caused by the heating. By constructing both curves, the regeneration curve can be used to define the extrapolated area and to correct for sensitivity change by comparing it with the additive dose curve. This works where the shapes of the curves differ only in scale (i.e., the sensitivity change is independent of dose). The curves are combined using the "Australian slide" method in a program developed by David Huntley of Simon Fraser University (Prescott et al. 1993). The equivalent dose is taken as the horizontal distance between the two curves after a scale adjustment for sensitivity change. Where the growth curves are not linear, they are fit to quadratic or cubic functions. Dose increments (usually five) are determined so that the maximum additive dose results in a signal about three times that of the natural and the maximum regeneration dose about five times the natural.

The inventory samples were processed before the Huntley program was purchased. Their growth curves were subsequently refit using the Huntley program. The later fit produced much better precision and these results were used in the determination of the final age.

A plateau region is determined by calculating the dose-intercept of additive and regeneration curves for 5-degree increments between 200°C and 450°C, and judging over which temperature range the intercepts do not differ significantly. The plateau region common to both curves, as well as the alpha growth curve, is integrated for analysis. (This procedure is no longer used in the laboratory. Instead equivalent dose using the slide method is determined at 10-degree increments. Where both procedures have been used, the intercept method has proved to be overly conservative in defining the plateau.)

Where the size of the sherd prevents a full multi-aliquot analysis, equivalent dose is determined by the SARA (single aliquot regeneration additive dose) technique (Mejdahl and Botter-Jensen 1994). Several aliquots are given additive doses, and then after heating to 450°C are given regeneration doses on the order of magnitude of the natural signal or the natural plus added dose signal. An apparent equivalent dose is determined from regeneration on each aliquot, but these are not accurate due to sensitivity changes. However, by plotting them against the original additive dose, a linear relationship results if the sensitivity change is independent of dose and an extrapolation to the dose axis provides the true equivalent dose.

Alpha Effectiveness

Alpha efficiency is determined by comparing additive dose curves using alpha and beta irradiations. The slide program is also used in this regard, taking the scale factor (which is the ratio of the two slopes) as the b-value (Aitken 1985).

Radioactivity

Radioactivity is measured by alpha counting in conjunction with atomic emission for ^{40}K. Samples for alpha counting are crushed in a mill to flour consistency, packed into plexiglass containers with ZnS:Ag screens, and sealed for one month before counting. The pairs technique is used to separate the U and Th decay series. For atomic emission measurements, samples are dissolved in HF and other acids and analyzed by a an IL spectrometer. K concentrations for each sample are determined by bracketing between standards of known concentration. Conversion to ^{40}K is by natural atomic abundance.

Both the sherd and an associated soil sample are measured for radioactivity. Additional soil samples are analyzed where the environment is complex, and gamma contributions determined by gradients (after Aitken 1985:Appendix H). Cosmic radiation is determined after Prescott and Hutton (1988). Radioactivity concentrations are translated into dose rates following Nambi and Aitken (1986) (which has since been updated by Adamiec and Aitken 1998).

No soil sample was available for UW251 and UW252. The external gamma dose rate derived at site LA 106199 was therefore used for these two sherds, on the assumption that the soils from the two sites are quite similar in composition.

Moisture Contents

Water absorption values for the sherds are determined by comparing the saturated and dried weights. Because of the arid climate, moisture contents were assumed to be 20±10 percent of these values. Soil moisture was assumed to be 5.8±.2 percent, typical for sandy textures (Brady 1974:196).

Results

Each sample was given a laboratory number. The number and provenience of each sherd are given in Table 84. Radioactivity results are given in Table 85, while dose rates are given in Table 86.

NN028296

Table 84. Samples and Provenience

UW Lab #	Site #	FS #	Ceramic Type	Context
			Inventory Samples	
142	LA 105483	3	Gobernador Polychrome	
143	LA 105530	15	Gobernador Polychrome	
144	LA 105428	5	Gobernador Polychrome	
145	LA 105479	1	Sandstone	
146	LA 105938	31	Dinetah Gray	
147	LA 83529	1	Dinetah Gray	
			Testing and Excavation Samples	
236	LA 106203	27	Jemez Black-on-white	Surface of shallow midden
237a	LA 105475	48	Dinetah Gray	Excavated artifact concentration
237b	LA 105475	48	Dinetah Gray	Excavated artifact concentration
238	LA 83529	4	Gobernador Polychrome	Midden
239	LA 79456	70	Dinetah Gray	Excavated artifact concentration
240	LA 105630	33	Dinetah Gray	Shallow midden deposit
241	LA 105428	19	Rio Grand matte paint	Artifact concentration
242	LA 105929	20	Gobernador Polychrome	Surface
243	LA 110278	8	Dinetah Gray?	Surface of shallow midden
244	LA 105930	21	Dinetah Gray?	Shallow midden deposit
245	LA 106199	43	Gobernador Polychrome	Shallow midden deposit
246	LA 106168	10	Dinetah Gray	Surface of small boulder enclosure
251	LA 55836	8	Jemez Black-on-white	Surface of Romine Canyon Ruin
252	LA 55836	12	Gobernador Polychrome	Surface of Romine Canyon Ruin
253	LA 11196	389	Sandstone	Fill of rockshelter
254	LA 11196	223	Sandstone	Base of burned rock pile

NN028297

Table 85. Radioactivity Data

Sample	Uranium (U) (ppm)	Thorium (Th) (ppm)	Potassium (K) (%)	Water Absorption (%)
		Inventory Samples		
UW142	6.10±.40	16.73±1.73	2.87±.01	7.0
Soil	2.22±.22	15.72±1.44	1.81±.02	
UW143	5.64±.35	11.66±1.42	2.47±.02	9.7
Soil	2.68±.22	12.72±1.27	1.88±.01	
UW144	4.99±.36	18.88±1.83	2.68±.02	17.6
Soil	6.02±.45	24.34±2.36	1.63±.02	
UW145	1.71±.13	4.61±.78	2.05±.06	5.8
Soil	2.06±.16	6.79±1.02	1.80±.04	
UW146	4.93±.30	8.21±1.25	2.03±.02	11.0
Soil	1.41±.32	36.13±2.48	2.55±.04	
UW147	4.39±.27	6.44±1.11	2.22±.03	12.8
Soil	3.63±.25	10.16±1.27	1.82±.01	
		Testing and Excavation Samples		
UW236	5.94±.36	10.00±1.46	1.43±.01	12.6
Soil	3.40±.23	8.87±1.23	1.25±.02	
UW237 (1)	4.18±.27	10.21±1.27	1.67±.02	11.5
UW237 (2)	2.29±.16	5.13±.89	1.60±.02	12.3
Soil	2.03±.20	13.35±1.5	1.70±.03	
UW238	5.10±.36	17.85±1.79	2.38±.23	8.5
Soil	2.56±.20	9.98±1.28	1.57±.02	
UW239	4.69±.30	9.87±1.29	1.56±.12	13.7
Soil	2.45±.22	13.35±1.52	1.76±.02	
UW240	3.72±.23	7.92±.99	1.72±.02	12.1
Soil	1.86±.14	6.26±.78	1.79±.01	
UW241	3.16±.25	12.70±1.52	1.67±.01	20.7
Soil	2.96±.30	21.25±2.00	1.61±.01	
UW242	4.06±.30	14.96±1.60	2.51±.17	13.2
Soil	3.01±.26	17.09±1.44	1.66±.01	
UW243	3.86±.26	10.05±1.36	1.35±.02	14.5
Soil	2.11±.19	12.53±1.25	1.77±.01	
UW244	3.20±.22	7.95±1.18	1.05±.01	12.9
Soil	2.39±.20	11.91±1.22	1.67±.03	
UW245	5.24±.37	16.69±1.84	2.77±.03	7.9
Soil	2.37±.19	9.44±1.26	1.35±.01	
UW246	3.20±.22	7.95±1.10	2.14±.02	10.1
Soil	1.40±.16	10.92±1.34	1.64±.02	
UW251	8.11±.52	21.61±2.14	2.31±.01	15.1
UW252	5.11±.33	12.55±1.57	2.55±.02	9.5
UW253	3.06±.23	11.69±1.22	1.23±.01	7.0
Soil	2.88±.22	10.82±1.39	1.32±.01	
UW254	1.02±.09	3.58±.61	1.94±.02	7.2
Soil	1.56±.17	10.39±1.32	1.87±.02	

ppm = parts per million

NN028298

Table 86. Dose Rates

Sample	Total (Gy/ka)	Alpha (%)	Beta (%)	Gamma (%)	Cosmic (%
			Inventory Samples		
UW142	7.97±.23	37.5	46.7	10.8	5.0
UW143	6.98±.22	37.8	45.3	11.0	5.7
UW144	7.77±.28	36.0	43.5	15.3	5.1
UW145	3.52±.12	14.2	58.8	15.3	11.4
UW146	6.10±.18	30.2	42.6	20.7	6.6
UW147	5.44±.18	32.0	48.0	13.1	7.4
			Testing and Excavation Samples		
UW236	5.57±.19	40.6	41.1	11.1	7.2
UW237a	4.90±.16	23.9	45.7	22.9	7.3
UW237b	3.86±.13	16.6	45.9	28.0	9.3
UW238	7.02±.31	34.2	45.4	15.1	5.3
UW239	5.15±.19	27.8	42.9	21.9	7.4
UW240	4.49±.15	24.5	47.9	18.3	8.5
UW241	4.68±.17	18.8	45.3	27.6	8.3
UW242	5.84±.21	26.4	51.9	14.9	7.0
UW243	4.74±.20	30.6	40.5	20.9	8.2
UW244	3.80±.14	24.7	40.3	25.0	10.3
UW245	6.94±.21	31.6	50.6	12.2	5.6
UW246	4.32±.12	20.6	56.3	13.7	9.3
UW251	7.23±.27	34.6	49.9	9.8	5.5
UW252	6.11±.18	31.3	51.9	10.3	6.5
UW253	3.03±.11	1.7	51.8	34.0	12.2
UW254	3.18±.11	4.4	54.4	30.5	10.4

Gy = grays; ka = 10,000 years

NN028299

External dose rate was also determined for three locations by inserting a $CaSO_4$: Dy dosimeter at the sample location and retrieving it one year later. The differences in external dose between that measured by the dosimeter and that measured by the sediment sample and the resulting differences in age are listed in Table 87. The differences in age are not significant, lending confidence to the sediment samples as good measures of the external dose rate.

Anomalous fading tests were run on all samples but UW237 and UW243 because of lack of sample and UW253 and UW254 because they consisted mostly of non-fading quartz. Only four sherds showed strong evidence of fading through time: UW236, UW244, UW245 and UW246. Figure 156 shows examples of sherds with and without evidence for fading. In strict sense, the derived ages from the fading sherds should be considered minimums, but given that their ages did not differ substantially from other non-fading sherds, the underestimation is believed to be insignificant.

Signal stability, as judged from the plateau tests, was generally satisfactory for all the samples. Figure 157 shows plateau tests for the additive dose, regeneration, and alpha growth curves for two samples, showing both wide and narrow plateau examples. For the sake of clarity, error bars are not shown. Plateaus chosen for analysis are given in Table 88.

Table 88 also shows other data relevant to equivalent dose. Figure 158 shows examples of the slide technique. The solid lines represent the fit to the regeneration points and the same fit shifted horizontally to align with the additive dose points. How well this second line fits the additive dose points is some indication of the goodness of fit of the slide. Where the fit is poor, some dose-dependent sensitivity change may be involved. The fits are generally satisfactory and scatter low with only discrepancies at high dose values for a few sherds (UW237A, UW237B, UW241). The best fits were generally cubic, indicating some supralinearity. In most cases there was no sensitivity change apparent, as indicated by the slope ratio of additive dose to regeneration, although for a few sherds and for both coarse grain analyses, some scaling was necessary to align the two curves. Figure 159 shows the slopes of the additive dose and alpha growth curves for two samples. Their ratio constitutes the b-value used to determine alpha efficiency. Again most of the fits were cubic.

Figure 160 shows examples of SARA data for sherds where this analysis was done. Up to eight aliquots were measured for each sherd. The equivalent doses are listed in Table 88. A comparison between these results and those obtained by the slide method is shown in Figure 161. While for most sherds the differences were insignificant, there seemed to be a systematic overestimation of equivalent dose using SARA (the dotted line in the figure represents perfect correlation, the solid line is a regression to the actual data), and two of the SARA values were significantly higher. The slide values, which also had much lower error terms, were therefore used in age determination. The reasons for the discrepancies are unclear.

Ages

Table 89 gives the derived ages. For the inventory samples, which were refit at a later date, ages from both the earlier and later fits are included. Note the much better precision with the later fits. The ages derived for the three samples where dosimeters were placed are also included.

Discussion and Conclusions

The age for UW254 reflects a significant residual geologic component since it well predates human habitation in the area. Any prehistoric use of the material did not include sufficient heating to completely reset the TL clock.

The precision of the dates, reflecting analytical errors only, ranged from 6.9 percent to 17.6 percent, with a mean of 10.3 percent. Better precision is not often obtained in luminescence dating, and the high precision here is attributed to low scatter in the growth curves. There was no tendency for better precision among different types of sherds or between surface and subsurface samples. The sherds from the immediate surface, with one exception (UW251), tended to be somewhat younger than those a few

Table 87. Dosimeter Comparisons

Location	Dosimeter (Gy/ka)	Sediment (Gy/ka)	Age Using Dosimeter (yr. A.D.)	Age Using Sediment (yr. A.D.)
LA 79456	1.400±.037	1.509±.099	1588 ± 67	1597 ± 66
LA 83529	1.409±.080	1.432±.094	1684 ± 26	1685 ± 28
LA 106199	1.567±.152	1.238±.088	1690 ± 22	1676 ± 22

[illegible] ka = 10,000 years

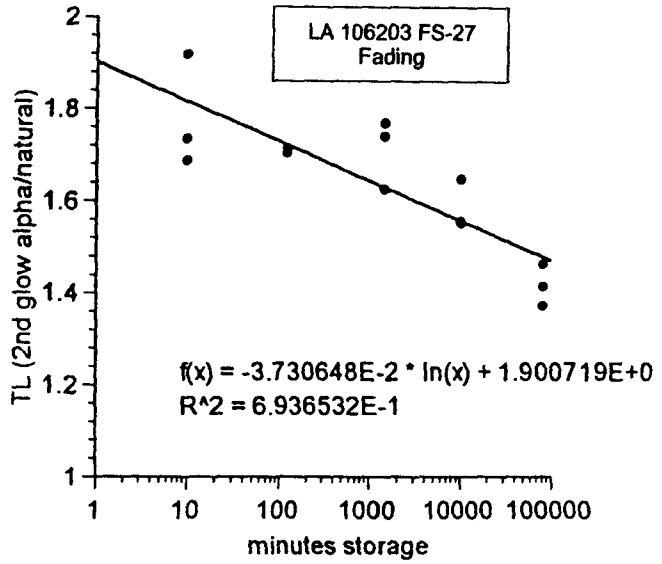

a. Sample #UW236

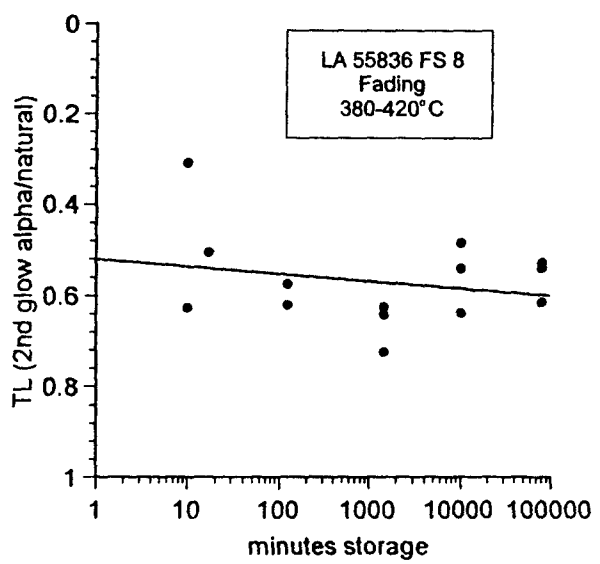

b. Sample #UW251

Figure 156. Results of anomalous fading test for two samples.

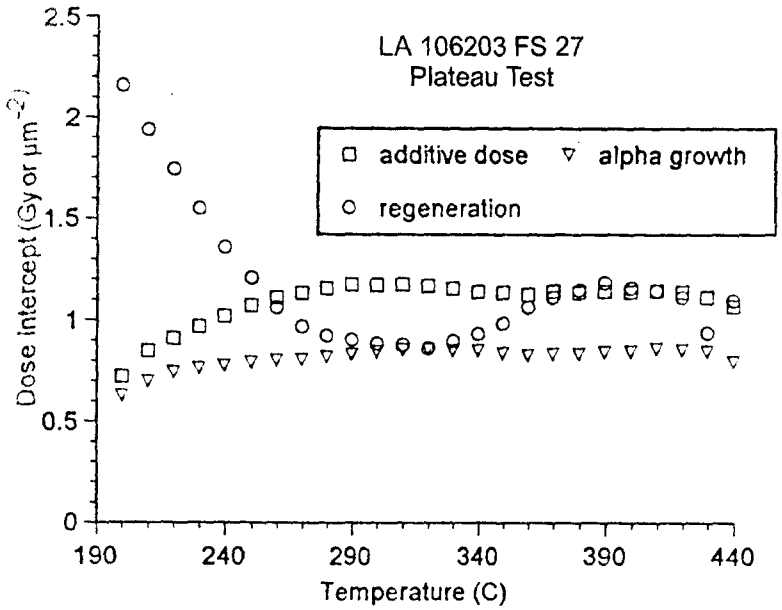

a. Sample #UW236

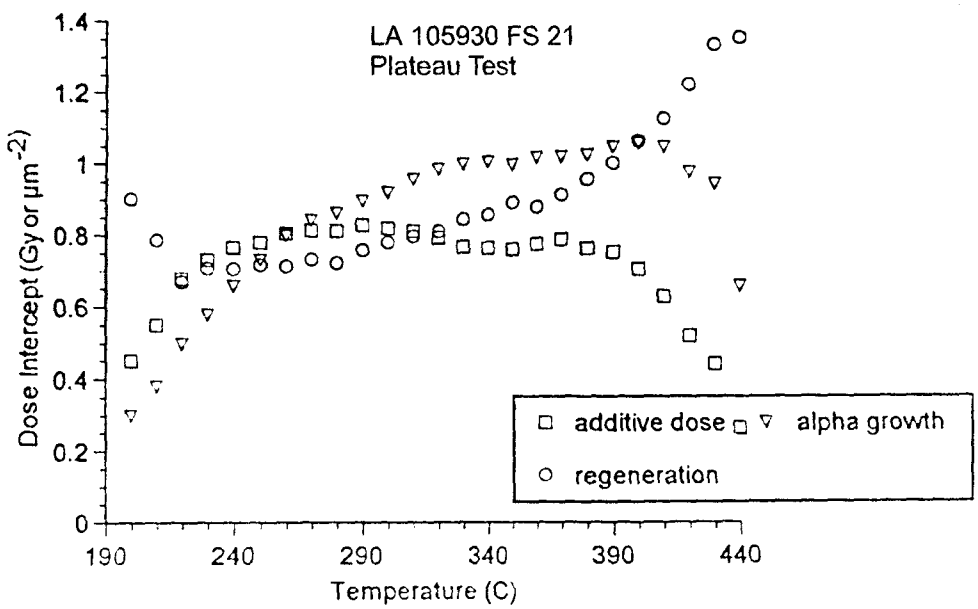

b. Sample #UW244

Figure 157. Plateau tests for two samples.

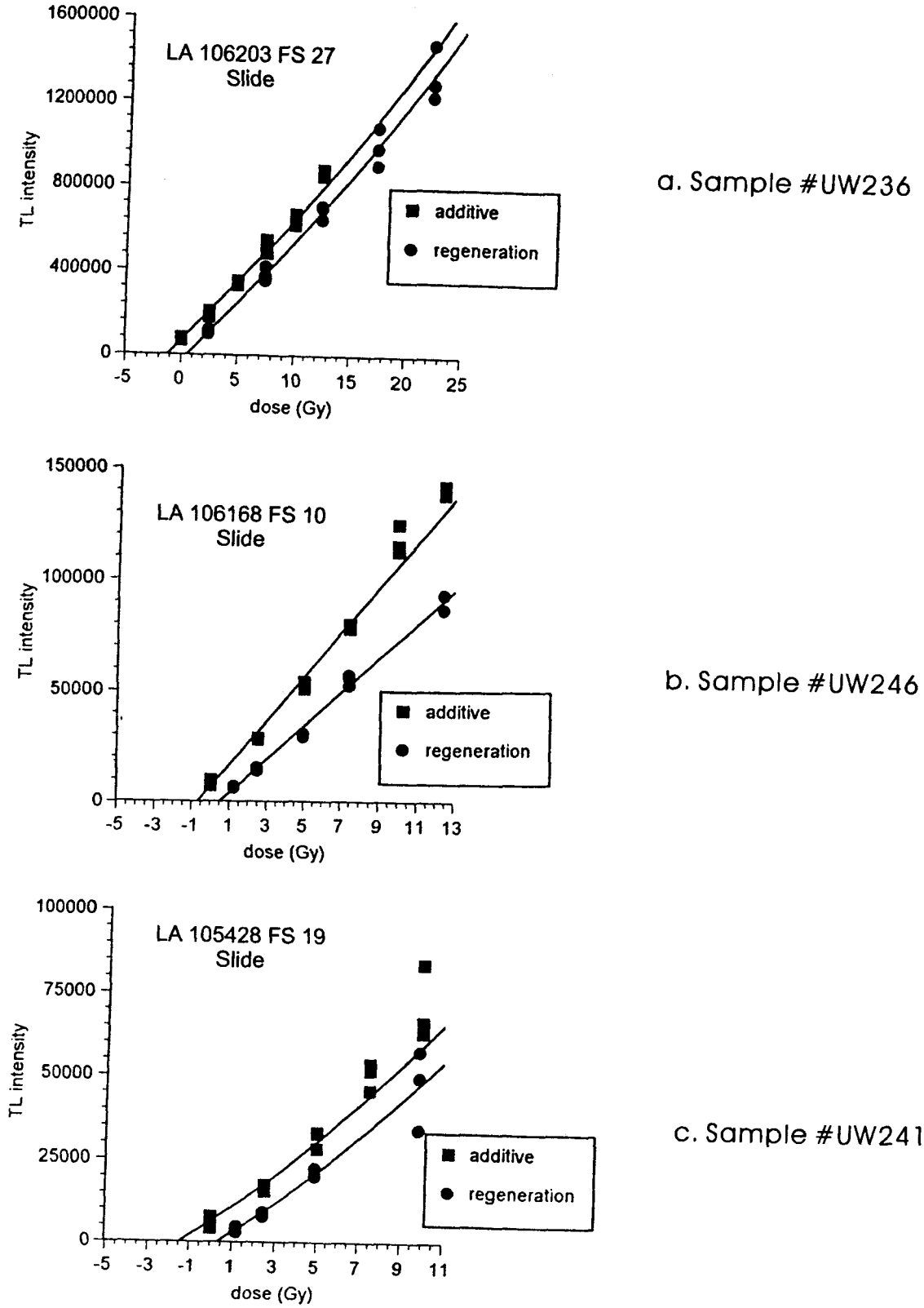

Figure 158. Growth curves for three samples.

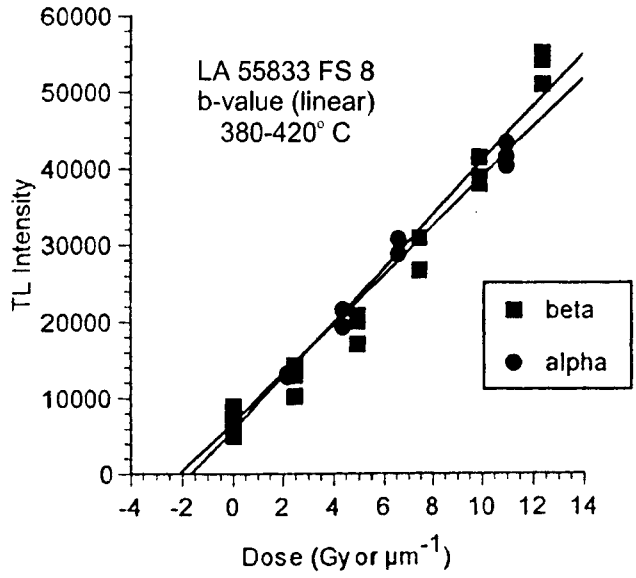

a. Sample #UW251

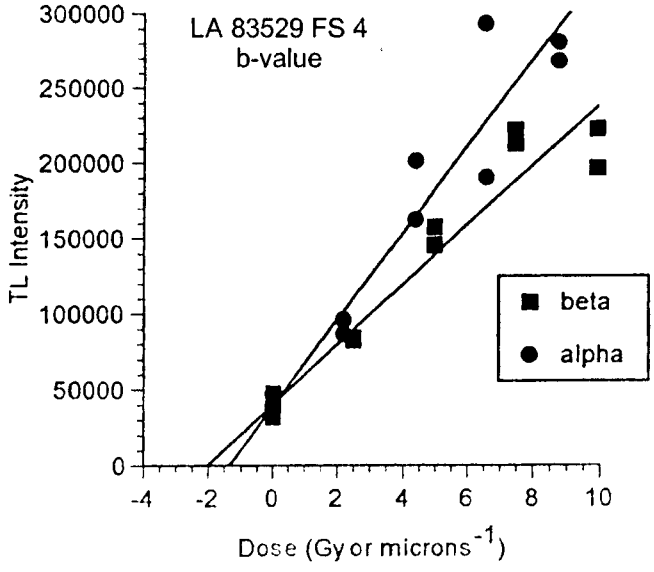

b. Sample #UW238

Figure 159. Two examples of differing slopes of additive dose curves using beta and alpha irradiation

Table 88. Plateaus and Equivalent Dose

Sample	Plateau (°C)	Slide fit	Sensitivity Change	Slide D_E (Gy)	b-value (Gy μm²)	$SARAD_E$ (Gy)
Inventory Samples						
UW142	270-350	linear	1.22±.04	1.99±.14	1.64±.07	-
UW143	260-310	linear	.89±.04	2.59±.21	1.77±.08	-
UW144	270-330	cubic	.77±.01	1.78±.22	1.66±.13	-
UW145	270-320	linear	1.0	1.16±.17	.99±.11	-
UW146	280-390	linear	1.45±.06	1.69±.12	1.53±.06	-
UW147	270-400	linear	.73±.05	1.42±.17	1.69±.11	-
Testing and Excavation Samples						
UW236	290-420	cubic	1.0	1.76± .09	1.56± .04	-
UW237a	280-420	linear	1.0	2.10± .16	1.00± .10	2.12±.92
UW237b	310-400	cubic	1.0	1.96± .18	1.04± .11	2.08± .90
UW238	330-410	cubic	1.0	2.19± .13	1.41± .12	2.88± .42
UW239	320-400	cubic	1.16± .12	2.06± .31	1.16± .08	2.03± .80
UW240	290-340	cubic	1.0	1.70± .14	1.11± .11	-
UW241	340-390	cubic	1.0	1.80± .14	.80± .07	2.13± .24
UW242	350-390	cubic	1.0	1.96± .10	1.12± .05	2.75± .42
UW243	320-380	cubic	1.0	1.65± .15	1.31± .17	1.95± .38
UW244	330-390	cubic	1.0	1.54± .13	1.04± .09	1.68± .52
UW245	240-310	cubic	1.0	2.23± .08	1.31± .07	-
UW246	300-350	cubic	1.31± .05	1.17± .08	.98± .04	-
UW251	380-420	cubic	1.0	3.66± .18	1.07± .10	-
UW252	340-380	cubic	1.32± .04	1.49± .25	1.32± .05	-
UW253	300-330	linear	.78± .09	1.40± .13	-	-
UW254	250-380	linear	.43± .11	61.2± 13.3	-	-

D_E = equivalent dose; Gy = grays; SARA = single aliquot regeneration additive dose

NN028305

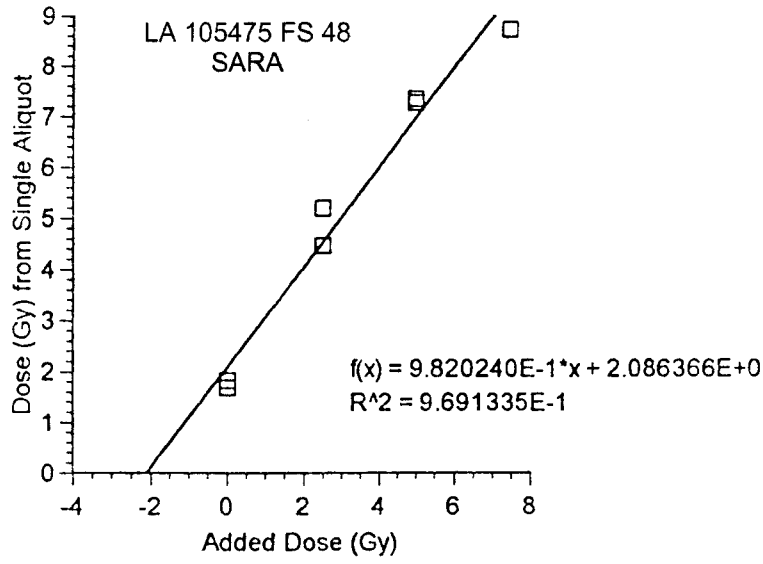

a. Sample #UW237a

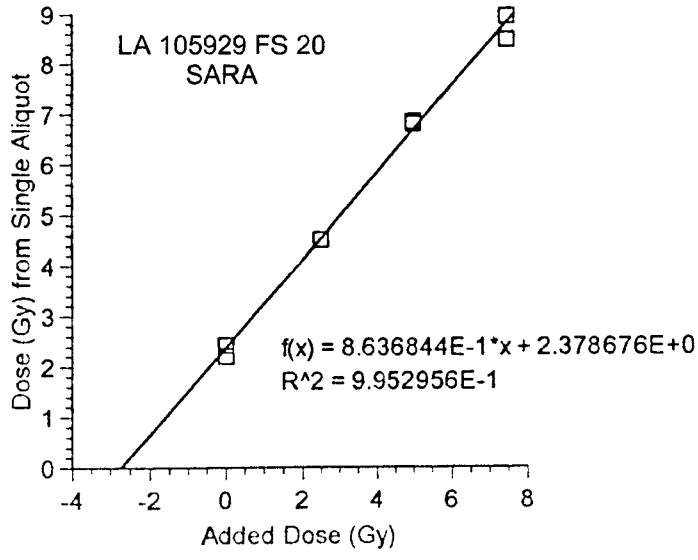

b. Sample #UW242

Figure 160. SARA results for two samples.

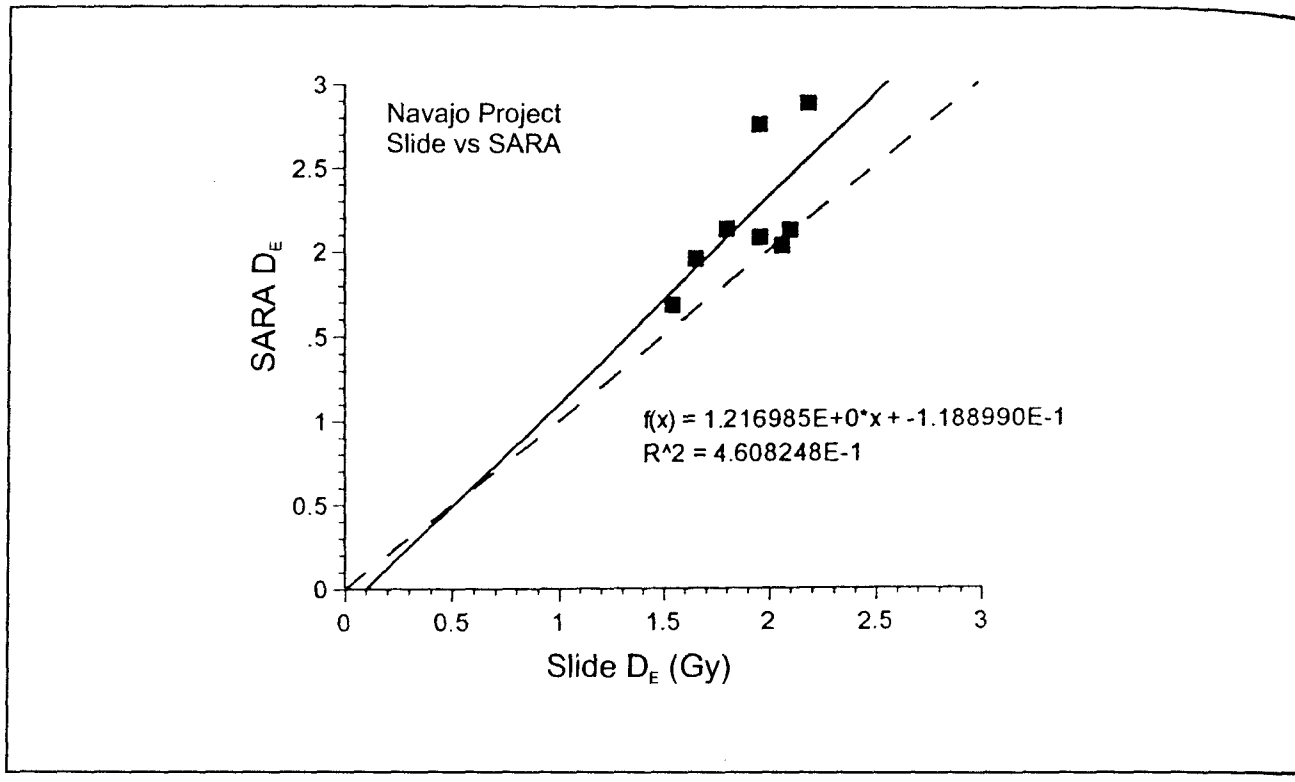

Figure 161. Comparison of equivalent doses from the slide and SARA techniques.

centimeters below the surface, perhaps because they were the latest deposited. Gray and reduced white wares (Dinetah and Jemez) tended to be older, while the polychromes tended to be younger, with a few exceptions. Two of the exceptions, U236 and U246, Jemez Black-on-white and Dinetah Gray, respectively, also suffered from anomalous fading which could explain their younger age. However, the other two fading samples produced ages similar to others of their kind. The sandstone samples that did not contain a geologic component dated in the same range as the gray and white wares with comparable precision.

The validity of the dates can be judged to some extent by comparison with independent dating. Several sites were also dated by tree rings. Although the tree rings and the TL dates reflect different events, the general agreement suggests overall validity for the luminescence dates and supports the use of luminescence dating for protohistoric ceramics from the Desert West (see Feathers and Rhode [1998] for similar results from Nevada, and Ramenofsky and Feathers [2002] for similar results from the Chama valley in the Rio Grande drainage). The comparisons are given in Table 90 (the tree ring ranges exclude some outliers) and discussed more fully in chapter 14.

The validity of the dates is explored in more detail in chapter 14, but as a prelude to that discussion, the results presented here appear to be reliable. The ages agree in general with independent dating data, and there seems to be no systematic error involved in using surface sherds. Validation of the surface ages is significant for CRM work because accurate dates can be obtained without destructive excavation. Luminescence dating should be applicable to most parts of the Southwest. Indeed, the University of Washington laboratory has produced more than 100 ceramic dates from the Southwest, including the Rio Grande drainage, the Colorado Plateau, and the Hohokam region of southern Arizona (Feathers 2001).

NN028307

Table 89. Summary of TL Dates from the Morris Site 1 Project

LA#	Lab No	Context	Sample Type	ReportedTL Date[a]	TL Date[a] (Improved Fit)	TL Date[a] (Dosimeter Adjusted)	TL Date Used in this Report[a]
11196	254	Subsurface	Sandstone	17271±4361B.C.	-	-	Not Used
11196	253	Subsurface	Sandstone	1535 ±49	-	-	1535 ±49
55836	251	Surface	Jemez B/W	1491 ±41	-	-	1491 ±41
55836	252	Surface	Gobernador Polychrome	1753 ±43	-	-	1753 ±43
79456	239	Subsurface	Dinetah Gray	1597 ±66	-	1588 ±67	1597 ±66
83529	147	Surface	Dinetah Gray	1782 ±123	1734 ±32	-	1734 ±32
83529	238	Subsurface	Gobernador Polychrome	1685 ±28	-	1684 ±26	1685 ±28
105428	144	Surface	Gobernador Polychrome	1797 ±54	1766 ±30	-	1766 ±30
105428	241	Subsurface	Rio Grande Matte Paint	1612 ±39	-	-	1612 ±39
105475	237a	Subsurface	Dinetah Gray	1569 ±41	-	-	1569 ±41
105475	237b	Subsurface	Dinetah Gray	1489 ±55	-	-	1489 ±55
105479	145	Surface	Sandstone	1685 ±158	1665 ±50	-	1665 ±50
105483	142	Surface	Gobernador Polychrome	1777 ±82	1745 ±19	-	1745 ±19
105530	143	Surface	Gobernador Polychrome	1680 ±51	1624 ±32	-	1624 ±32
105630	240	Subsurface	Dinetah Gray	1615 ±38	-	-	1615 ±38
105929	242	Subsurface	Gobernador Polychrome	1661 ±27	-	-	1661 ±27
105930	244	Subsurface	Dinetah Gray	1592 ±42	-	-	1592 ±42
105938	146	Surface	Dinetah Gray	1748 ±74	1718 ±21	-	1718 ±21
106168	246	Subsurface	Dinetah Gray	1726 ±24	-	-	1726 ±24
106199	245	Subsurface	Gobernador Polychrome	1676 ±22	-	1690 ±22	1676 ±22
106202	236	Surface	Jemez B/W	1681 ±26	-	-	1681 ±26
110278	243	Subsurface	Dinetah Gray	1649 ±39	-	-	1649 ±39

[a] = Years A.D. unless otherwise noted

Table 90. TL Versus Tree-ring Dates

Sample	TL Date (years A.D.)	Tree-ring range (years A.D.)
UW253	1535 ± 49	1698
UW251	1491 ± 41	1673 - 1723
UW252	1753 ± 43	1673 - 1723
UW238	1685 ± 28	1652 - 1748
UW147	1734 ± 32	1652 - 1748
UW144	1766 ± 30	1728
UW241	1612 ± 39	1728
UW145	1665 ± 50	1679 - 1730
UW142	1745 ± 19	1629 - 1740
UW143	1624 ± 32	1689 - 1719
UW240	1615 ± 38	1644 - 1915
UW244	1592 ± 42	1666 - 1695
UW245	1676 ± 22	1731 - 1750
UW243	1649 ± 39	1699
UW242	1661 ± 27	1695

NN028309